TASK QUARTERLY 6 No 3 (2002), 437–446

A NON-LOCAL ELASTO-PLASTIC MODEL TO DESCRIBE LOCALISATIONS OF DEFORMATION IN CONCRETE

JERZY BOBIŃSKI[1,2] AND JACEK TEJCHMAN[1]

[1] *Civil Engineering Faculty, Gdansk University of Technology, Narutowicza 11/12, 80-952 Gdansk, Poland*
tejchmk@pg.gda.pl

[2] *Academic Computer Centre in Gdansk TASK, Narutowicza 11/12, 80-952 Gdansk, Poland*
bobin@task.gda.pl

(Received 24 May 2002)

Abstract: The paper presents numerical simulations of behaviour of concrete elements subjected to uniaxial compression for plane strain. FE-calculations are performed with two different elasto-plastic constitutive laws for concrete. Numerical results obtained suffer from mesh sensivity due to the presence of material softening. To obtain a well-posed boundary problem and a mesh independent solution, conventional constitutive laws with softening require an extension (called regularisation) to describe properly the localisations of deformations. In this paper elasto-plastic constitutive laws are extended by non-local strain terms. Owing to them, localisations of deformations are realistically captured.

Keywords: concrete, localisation, non-local theory, elasto-plasticity, characteristic length

1. Introduction

The phenomenon of localisation of deformation occurs in many engineering materials like metals, soils, polimers and concrete. In the case of localisation, deformations are concentrated in a small region of the material, whereas in the remaining part they are negligible. Due to the localisation of deformation, a degradation of the material strength develops (second-order work is negative). The localisations can occur as:

- cracks (if cohesive properties of the material dominate over frictional ones) or
- shear bands (if frictional properties are crucial).

Classical FE-analyses of the behaviour of material with softening are not able to describe properly both the thickness of localisation zones and distance between them. They suffer, namely, from mesh sensivity (its size and alignment), Bažant [1], de Borst [2]. They produce, thus, unrealiable results: localisations become

narrower upon mesh refinement, and computed force-displacement curves depend on the thickness of localisations (in particular in a post-peak regime). The reason is that differential equations of motion change their type (for static calculations from elliptic to hyperbolic) and the boundary problem is mathematically ill-posed (de Borst *et al.* [3]). In this case, deformations tend to localise in zero-thickness zones when using analytical calculations or in one-element wide bands by FE-modeling. Thus, classical constitutive models require an extension in the form of a characteristic length to describe (regularize) the thickness and distance of localisations.

One of the regularisation techniques is to include viscosity in the constitutive model. Time derivatives of velocity of strains are added to equations of motion (Loret and Prevost [4], Sluys and de Borst [5]). This method is useful in dynamic calculations. For quasi-static problems, the amount of viscosity required to obtain a proper regularisation is often too high from a physical point of view (Sluys and de Borst [5]).

Another method of regularisation is to use a polar constitutive law laid down within a Cosserat continuum (Cosserat and Cosserat [6]). The rotational degrees-of-freedom (independent from displacement degrees-of-freedom) are extra introduced into a classical continuum theory. Curvatures (the spatial derivatives of rotations) are connected to couple stresses. The deformation and stress tensor are non-symmetric. The Cosserat continuum was applied first as a regularisation technique in an elasto-plastic formulation by Mühlhaus [7]. Later this model has been used by Tejchman and Wu [8], de Borst [9], Tejchman *et al.* [10] to model shear localisations in granular bodies where pronounced rotations of grains take place.

The next way of regularisation is a strain gradient model. In this model, additional higher-order spatial derivatives of strains are included in constitutive equations (Schreyer and Chen [11], Zbib and Aifantis [12], Mühlhaus and Aifantis [13], de Borst and Mühlhaus [14] and Sluys [15]).

The other way of regularisation is a non-local model (Eringen [16, 17]). The model can be considered as a generalization of a strain gradient model with second-order strain gradient terms (Mülhaus and Aifantis [13], de Borst and Mühlhaus [14]). In this model, a strain measure depends not only on the plastic strain in the material point considered but also on the plastic strain around the point (Bažant *et al.* [18]). The remaining general stresses and strains are usually local. The non-local model has been used next by Brinkgreve [19], Chen [20], Strömberg and Ristinmaa [21], Marcher and Vermeer [22].

In this paper, the results of FE-calculations of a concrete specimen subjected to uniaxial compression with two elasto-plastic models (with and without regularisation) are demonstrated. The FE-analysis was carried out with an elasto-plastic law by Drucker-Prager and von Mises. An elasto-plastic by von Mises was extended by non-local terms according to a Brinkgreve's proposal [19].

2. Constitutive models for concrete

2.1. Drucker-Prager yield criterion

One of two models for concrete defined in *Abaqus* package is an inelastic concrete model [23, 24]. This model is designed for concrete elements subjected to essentially

monotonic straining at low confining pressures. It uses isotropic hardening with an associated flow rule. It enables to define material softening in compressive and tensile region. Concrete model is fully defined with the following parameters and material functions:

- modulus of elasticity,
- Poisson's ratio,
- stress-strain curve in uniaxial compression,
- stress-strain curve in uniaxial tension,
- the ratio of the ultimate biaxial compressive stress to the ultimate uniaxial compressive stress r_{bc}^{σ},
- the absolute value of the ratio of the uniaxial tensile stress at failure to the ultimate uniaxial compressive stress,
- the ratio of the magnitude of a principal component of plastic strain at ultimate stress during biaxial compression to plastic strain at ultimate stress in uniaxial compression r_{bc}^{ε},
- the ratio of the tensile principal stress at cracking in plane stress (when the other principal stress is at the ultimate compressive value) to the tensile cracking stress under uniaxial tension r_f,
- shear coefficient after cracking ρ^c.

In a compression region, concrete is modeled by a Drucker-Prager yield surface ("compression" surface in Figure 1):

$$f_c = q - \sqrt{3}a_0 p - \sqrt{3}\tau_c = 0,$$

where $p = -tr(\sigma_{ij})/3$ is the mean stress, $q = \sqrt{\frac{3}{2}s_{ij}s_{ij}}$ – the equivalent deviatoric stress measure, s_{ij} – the deviatoric stress, a_0 – the constant and τ_c – the hardening (cohesive) parameter assumed from the relation stress-strain for uniaxial compression. In a tensile region, a crack detection surface is equal to (Figure 1):

$$f_t = q' - \left(3 - b_0\frac{\sigma_t}{\sigma_t^u}\right)p' - \left(2 - \frac{b_0}{3}\frac{\sigma_t}{\sigma_t^u}\right)\sigma_t = 0,$$

where σ_t^u is the failure stress in uniaxial tension, b_0 – the material constant, σ_t – the hardening parameter in tension, p' and q' – the values defined as p and q for compression (but without stress components associated with open cracks). The flow rule is defined as:

$$d\varepsilon_{ij}^p = d\lambda\frac{\partial g}{\partial \sigma_{ij}},$$

where ε_{ij}^p is the plastic strain increment tensor, $d\lambda$ is the plastic multiplier and g is the potential function. By using associated flow rule, $f = g$.

To calculate the displacement u_0 at stress in tension equal to zero, the fracture energy G_f, required to open a crack of an unit area, is assumed as a material constant (Hilleborg [25]):

$$u_0 = \frac{2G_f}{\sigma_t^u}.$$

Concrete tensile behaviour after cracking is described by the stress evolution versus the displacement in the localisation zone. To compute this displacement, calculated global strain is multiplied by a characteristic length associated with the size of finite

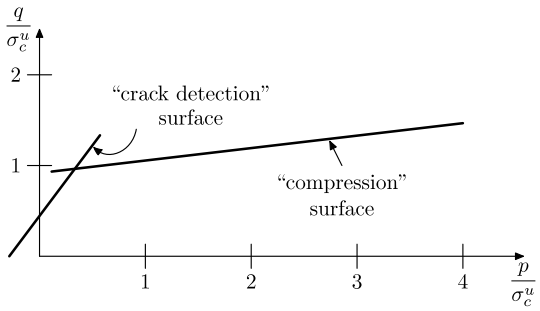

Figure 1. Concrete failure surfaces in the $p-q$ plane (σ_c^u – ultimate uniaxial compressive stress)

elements. For planar elements, the characteristic length is equal to the square root of the integration point area and for solid elements it is equal to the cube root of the integration point volume. The main advantage of this model is the ability to describe the concrete behaviour under monotonic loading in a realistic way (Kupfer and Gerstle [26]) with only 9 material constants.

2.2. Von Mises yield criterion

The second constitutive model used in FE-calculations is an elasto-plastic one by von Mises with isotropic hardening and softening. The yield function f and potential function g are defined as:

$$f(q,\kappa) = g = q - \sigma_0(\varepsilon_p),$$

where q is the Mises equivalent deviatoric stress, σ_0 is the equivalent strength and ε_p denotes the equivalent plastic strain ($\varepsilon_p = \sqrt{\frac{2}{3} e_{ij}^p e_{ij}^p}$) used as a measure of hardening and softening (e_{ij}^p – plastic deviatoric strain tensor).

3. Non-local approach

As a regularisation technique to describe localisations of deformation in material with softening, a non-local approach is used. The aim of a non-local approach is to obtain a well-posed boundary value problem, to ensure mesh independence and to promote convergence of numerical procedures. In this approach, average stresses σ_{ij}^* and average strains ε_{ij}^* are defined as:

$$\sigma_{ij}^*(x_n) = \frac{1}{A}\iiint w(x'_n)\sigma_{ij}(x_n + x'_n)dx'_1dx'_2dx'_3,$$

$$\varepsilon_{ij}^*(x_n) = \frac{1}{A}\iiint w(x'_n)\varepsilon_{ij}(x_n + x'_n)dx'_1dx'_2dx'_3,$$

where a superimposed star denotes a non-local mode, x_n is a global, x'_n is a local coordinate with $n = 1,2,3$, w is a weighting function, σ_{ij}, ε_{ij} – local stresses and strains in the entire body and A is a weighted volume:

$$A = \iiint w(x'_n)dx'_1dx'_2dx'_3.$$

The integral of the function w over the domain r must be equal to 1:

$$\int_{\infty}^{\infty} w(r)dr = 1.$$

Usually, the error function is taken as a weighting function w [19]:

$$w(r) = \frac{1}{l\sqrt{\pi}} e^{-(\frac{r}{l})^2}, \tag{1}$$

where r is a distance from the considered point to all points of the body and l is a characteristic (internal) length related to the width of the localisation zone. The averaging is, thus, restricted to a small representative area around the material point considered. In homogenous bodies, the non-locality can be related only to the equivalent plastic strain measure ε_p^* in the softening regime (Bažant [18]):

$$\varepsilon_p^*(x) = \frac{1}{A}\int_V w(r)\varepsilon_p(x+r)dV. \tag{2}$$

According to a Brinkgreve's proposal [19] (see also Strömberg [21]), the non-local variable ε_p^* can be defined as:

$$\varepsilon_p^*(x) = (1-\alpha)\varepsilon_p(x) + \frac{\alpha}{A}\int_V w(r)\varepsilon_p(x+r)dV, \tag{3}$$

where α is a parameter. This formulation consists of a local and a purely non-local part. It turned out to be more effective (for $\alpha > 1$) to describe localisations than the formulation including only a non-local part [19]. For $\alpha = 0$, a classical (local) theory is obtained, and for $\alpha = 1$, Equation (2) is recovered. To simplify calculations (de Borst and Mühlhaus [14]), plastic strain rates can be approximated by total strain rates:

$$d\varepsilon_p^*(x) \approx d\varepsilon_p(x) + \alpha\left(\frac{1}{A}\int_V w(r)d\varepsilon(x+r)dV - d\varepsilon(x)\right),$$

where $d\varepsilon_p$ is the plastic and $d\varepsilon$ is the total increment of the equivalent strain.

4. Numerical calculations

Numerical calculations were performed for plane strain using a concrete specimen 15cm wide and 30cm high subject to uniaxial compression (Figure 2a). All nodes at the lower edge were fixed in vertical direction. To preserve the stability of the specimen, the node in the middle of the lower edge was kept fixed. The deformations were initiated through constant vertical displacement increments prescribed to nodes along the upper edge of the specimen. The lower and upper edges were smooth. To investigate the effect of the mesh on the results, various discretisations were used: coarse (5×10), medium (10×20) and fine (15×30) where each quadrilateral is composed of four diagonally crossed triangular elements, with linear shape functions. The localisation was induced by a small material imperfection at the lower left corner of the specimen (Figure 2b).

To solve a non-linear equation system, the full Newton method was applied for local constitutive laws, and the modified Newton-Raphson scheme with an elastic stiffness matrix for a non-local constitutive law. A geometric nonlinearity was included. Cauchy stresses and logarithmic strains were used. At least 1000 increments were required to obtain a vertical displacement of the top, $\Delta v = 1.5$mm.

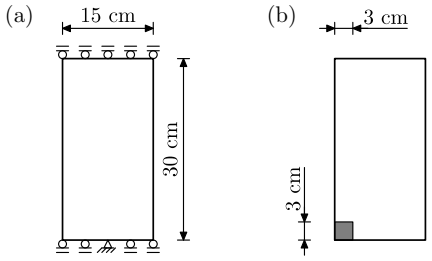

Figure 2. Uniaxial concrete compression: (a) geometry and boundary conditions of the specimen, (b) location of imperfection

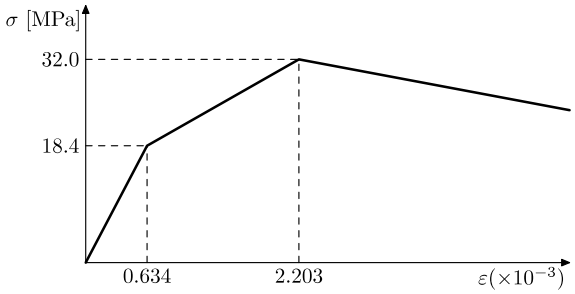

Figure 3. Stress–strain curve for concrete in uniaxial compression

In an elasto-plastic constitutive law by Drucker-Prager, the Young modulus was taken as $E = 29\text{GPa}$ and Poisson's ratio as $\nu = 0.18$. The stress-strain curve in uniaxial compression assumed for calculations is shown in Figure 3 (softening modulus $H = 1.5\text{GPa}$). The compressive strength of the concrete specimen is 32MPa at $\varepsilon = 2.2‰$ and the residual concrete strength is 12MPa. The strength in uniaxial tension is assumed to be $\sigma_t^u = 2.4\text{MPa}$. To model the behaviour of concrete in tension, the displacement u_0 was taken as $7 \cdot 10^{-5}\text{m}$. This value is equivalent to the fracture energy $G_f = 84\text{kN/m}$. Other material constants were chosen as: $r_{bc}^{\sigma} = 1.16$, $r_{bc}^{\varepsilon} = 1.28$, $r_f = 0.33$ and $\rho^c = 1.0$. The imperfection in the model was introduced in this way that the maximum strength of concrete during uniaxial compression was diminished by 2%.

Figures 4 and 5 present the results: deformed meshes for different discretisations (deformation scale factor is equal to 6.0) and load-displacement diagrams. The deformations localise in one element wide shear band with the inclination of 45° which is equal to the mesh alignment. A severe mesh-dependency is obtained since the thickness of the shear zone decreases with decreasing element size. The maximum equivalent plastic strains occur in three elements across the shear band (grey color indicates elements with larger strains). In the load-displacement diagram (Figure 5), the vertical force denotes the sum of all vertical nodal forces along the top and the displacement is related to the displacement of the top edge. The curves for all meshes are similar up to the peak. The maximum force is equal to $P_{\max} = 6.18 \cdot 10^3\text{kN}$ for the vertical displacement $v_{\max} \approx 1\text{mm}$. After the peak, the evolution of the vertical force depends on the mesh. A strong unstable failure mechanism occurs.

The FE-results with an elasto-plastic law by von Mises are shown in Figures 6 and 7. Similar material parameters were assumed. Figure 6 shows deformed meshes

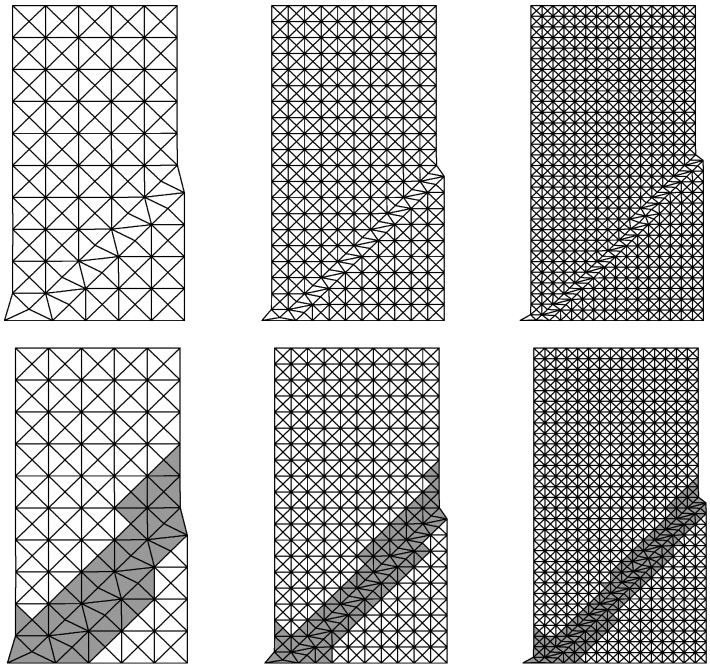

Figure 4. Deformed meshes and equivalent plastic strains for different discretisations using an elasto-plastic model by Drucker-Prager (without regularisation)

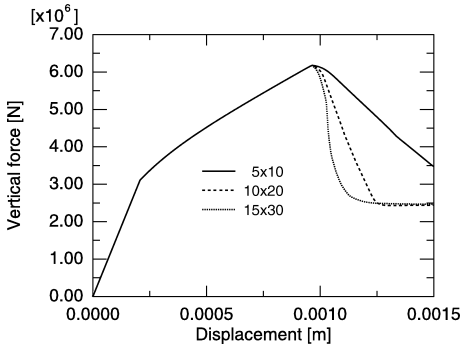

Figure 5. Load–displacement diagrams for different mesh discretisations (Drucker-Prager criterion without regularisation)

and equivalent plastic strains. The deformations and strains localise again in one element wide shar band with the inclination of 45°. The maximum vertical force along the top is equal to $P_{\max} = 5.45 \cdot 10^3$ kN for the displacement $v_{\max} = 0.66$ mm. The load-displacement curves are again equal in a pre-peak regime and differ significantly after the peak (Figure 7). For a medium and fine mesh, the strength degradation is very sharp.

Figures 8 and 9 demonstrate the FE-results with a non-local elasto-plastic constitutive law by von Mises. Two additional constants were taken into account: the parameter α and the characteristic length l (Equation (1)) both determining the width of the localisation zone. The calculations were performed with the parameter α changing from 1 to 4 and the parameter l changing from 2cm to 10cm. Deformed

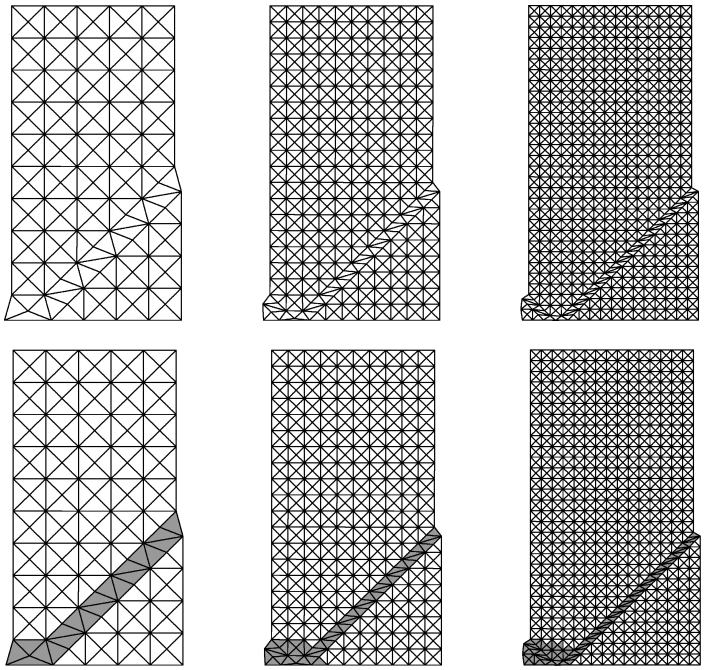

Figure 6. Deformed meshes and equivalent plastic strains for different discretisations using an elasto-plastic model by von Mises (without regularisation)

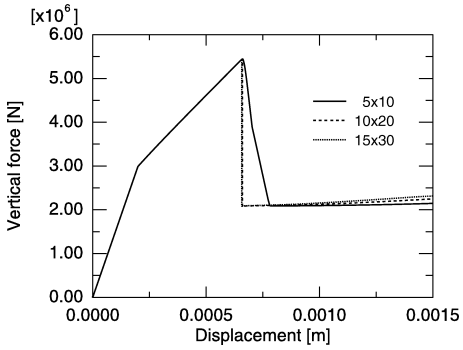

Figure 7. Load–displacement diagrams for different mesh discretisations (von Mises criterion without regularisation)

meshes and equivalent plastic strains for $\alpha = 2$ and $l = 3$cm are shown in Figure 8. Deformations localise in a band wider than one finite element. The thickness of the shear zone is approximately 7cm ($\approx 2l$) and does not depend upon the mesh size. The load-displacement diagrams are presented in Figure 9. The maximum load is the same as in a local model (Figure 7). The evolution of the vertical force along the top after the peak is the same for all discretisations. The results show that the thickness of the localised shear zone increases with increasing parameters α and l. The thickness is approximately equal to αl. The maximum vertical load is independent of α and l. The material softening decreases with increasing l. For $\alpha = 1$, the model is less effective to describe the thickness of the localisation zone.

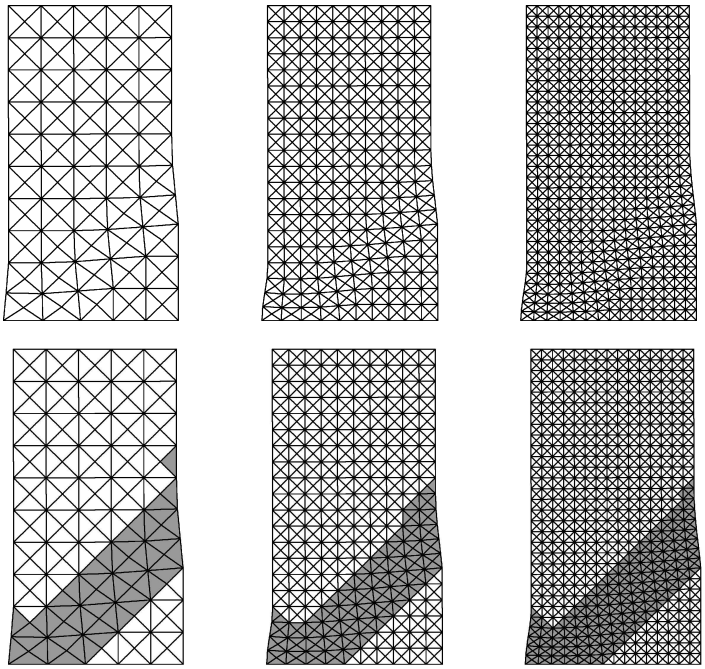

Figure 8. Deformed meshes and equivalent plastic strains for different discretisations using an elasto-plastic model by von Mises (with regularisation)

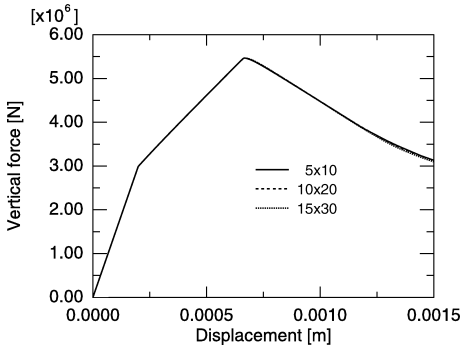

Figure 9. Load–displacement diagrams for different mesh discretisations (von Mises criterion with regularisation)

5. Conclusions

FE-calculations demonstrate that conventional elasto-plastic models suffer from mesh-dependency. The thickness and the inclination of shear zones, and the load-displacement diagram in the post-peak regime depend strongly on the mesh discretisation. The addition of a non-local strain measure results in a full regularisation of the boundary value problem. Numerical results converge to a finite size of localisation upon mesh refinement. The thickness of localised zones increases with an increase of a characteristic length.

The numerical study on localisations of deformation in concrete will be continued. An elasto-plastic constitutive law by Drucker-Prager will be extended by a non-

local plastic strain measure. The characteristic length will be identified with the mean size of aggregate.

Acknowledgements

The numerical calculations were performed on supercomputers of Academic Computer Centre in Gdansk TASK.

References

[1] Bažant Z P 1976 *ASCE J. Eng. Mech.* **102** 331
[2] de Borst R 1986 *Non-linear Analysis of Frictional Materials*, Dissertation, Delft University of Technology
[3] de Borst R, Mülhaus H B, Pamin J and Sluys L Y 1992 *Proc. 3rd Int. Conf. Comput. Plasticity*, Pineridge Press, Swansea, Wales, U.K., pp. 483–508
[4] Loret B and Prevost J H 1990 *Comp. Appl. Mech. Eng.* **83** 247
[5] Sluys L J and de Borst R 1991 *Proc. Conf. on Fracture Processes in Concrete, Rock and Ceramics* (Van Mier J, Rots J G and Bakker A, Eds.), Chapman and Hall, London, pp. 661–671
[6] Cosserat E and Cosserat F 1909 *Théorie des Corps Deformables*, Herman et fils, Paris
[7] Mühlhaus H B 1986 *Ing. Arch.* **56** 389
[8] Tejchman J and Wu W 1993 *Acta Mechanica* **99** 61
[9] de Borst R 1990 *Proc. 2nd Int. Conf. Computer Aided Analysis and Design of Concrete Structures* (Bicanic N and Mang H A, Eds.), Pineridge Press, Swansea, U.K., pp. 931–944
[10] Tejchman J, Herle I and Wehr J 1999 *Int. J. Num. Anal. Meth. Geomech.* **23** 2045
[11] Schreyer H L and Chen Z 1986 *J. Appl. Mech.* **53** 791
[12] Zbib H M and Aifantis C E 1989 *Appl. Mech. Rev.* **42** (11) 295
[13] Mühlhaus H B and Aifantis E C 1991 *Int. J. Solids Structures* **28** 845
[14] de Borst R and Mühlhaus H B 1991 *Proc. 4th Int. Conf. on Nonlinear Eng. Comp.* (Bićanić N, Marović P, Owen D R J, Jović V and Mihanović A, Eds.), Pineridge Press, Swansea, U.K., pp. 239–260
[15] Sluys L J 1992 *Wave Propagation, Localisation and Dispersion in Softening Solids*, Dissertation, Delft University of Technology
[16] Eringen A C 1972 *Int. J. Engng. Sci.* **10** 1
[17] Eringen A C 1981 *Int. J. Engng. Sci.* **19** 1461
[18] Bažant Z P, Lin F B and Pijaudier-Cabot G 1987 *Proc. Int. Conf. Comput. Plasticity* (Owen, Hinton and Onate, Eds.), Barcelona, pp. 1757–1780
[19] Brinkgreve R B J 1994 *Geomaterial Models and Numerical Analysis of Softening*, Dissertation, Delft University of Technology
[20] Chen E P 1999 *Int. J. Num. Anal. Meth. Geomech.* **53** 1
[21] Strömberg L and Ristinmaa M 1996 *Comp. Meth. Appl. Mech. Engng.* **136** 127
[22] Marcher T and Vermeer P A 2001 *Continuous and Discontinuous Modelling of Cohesive-Frictional Materials* (Vermeer P A *et al.*, Eds.), Springer-Verlag, pp. 89–110
[23] 2000 *Abaqus Standard User's Manual* Vol. 1 version 6.1, Hibbit, Karlsson and Sorensen Inc.
[24] 2000 *Abaqus Theory Manual* version 6.1, Hibbit, Karlsson and Sorensen Inc.
[25] Hilleborg A, Modeer M and Petersson P E 1976 *Cement and Concrete Research* **123** (2) 773
[26] Kupfer H B and Gerstle K H 1973 *J. Engng. Mech. Div. ASCE* **99** 853